J. Cell. Mol. Med. Vol 14, No 3, 2010 pp. 587-599

Non-viral $VEGF_{165}$ gene therapy – magnetofection of acoustically active magnetic lipospheres ('magnetobubbles') increases tissue survival in an oversized skin flap model

Thomas Holzbach [a], Dialekti Vlaskou [b], Iva Neshkova [a], Moritz A. Konerding [c], Klaus Wörtler [d], Olga Mykhaylyk [b], Bernd Gänsbacher [b], H.-G. Machens [a], Christian Plank [b], Riccardo E. Giunta [a, *]

[a] Department of Plastic Surgery and Hand Surgery, Munich, Germany
[b] Institute of Experimental Oncology, Munich, Germany
[c] Institute of Anatomy and Cell Biology, Johannes Gutenberg University, Mainz, Germany
[d] Department of Radiology, Technische Universität München, Munich, Germany

Received: June 10, 2008; Accepted: October 30, 2008

Abstract

Adenoviral transduction of the VEGF gene in an oversized skin flap increases flap survival and perfusion. In this study, we investigated the potential of magnetofection of magnetic lipospheres containing $VEGF_{165}$-cDNA on survival and perfusion of ischemic skin flaps and evaluated the method with respect to the significance of applied magnetic field and ultrasound. We prepared perfluoropropane-filled magnetic lipospheres ('magnetobubbles') from Tween60-coated magnetic nanoparticles, Metafectene, soybean-oil and cDNA and studied the effect in an oversized random-pattern-flap model in the rats ($n = 46$). VEGF-cDNA-magnetobubbles were administered under a magnetic field with simultaneously applied ultrasound, under magnetic field alone and with applied ultrasound alone. Therapy was conducted 7 days preoperative. Flap survival and necrosis were measured 7 days post-operatively. Flap perfusion, VEGF-protein concentration in target and surrounding tissue, formation and appearance of new vessels were analysed additionally. Magnetofection with VEGF-cDNA-magnetobubbles presented an increased flap survival of 50% and increased flap perfusion ($P < 0.05$). Without ultrasound and without magnetic field, the effect is weakened. VEGF concentration in target tissue was elevated ($P < 0.05$), while underlying muscle was not affected. Our results demonstrate the successful VEGF gene therapy by means of magnetobubble magnetofection. Here, the method of magnetofection of magnetic lipospheres is equally efficient as adenoviral transduction, but has a presumable superior safety profile.

Keywords: VEGF • gene therapy • angiogenesis • magnetofection • magnetobubbles • lipospheres • magnetic

Introduction

Blocking the angiogenic cascade is an important objective in limiting tumour growth, ocular neovascularization or arthritis; however, a wide range of applications in the field of reconstructive surgery require the induction of angiogenesis. A mended vascular network and improved blood flow will be beneficial to all kinds of flap designs and chronic wounds. Necrosis in critically perfused tissue could be minimized and targeted angiogenesis will result in greater liberty of flap design [1].

Impaired wound healing is a common post-operative complication and insufficient supply of oxygen and nutrients to the tissue impedes the physiological phases of healing. The formation of necrosis additionally deteriorates the nutrient supply, averts the formation of granulation tissue and promotes the colonization of bacteria. An improved vascular network would not only accelerate wound healing but also reduce the necessity of frequent surgical interventions.

Methods to promote angiogenesis and improve local perfusion have been investigated for many years, and of the different growth factors involved VEGF has proved to be among the most promising. The clinical deployment of VEGF gene therapy in phase II clinical trials is so far limited to the treatment of myocardial

*Correspondence to: Riccardo E. GIUNTA, M.D.,
Department of Plastic Surgery and Hand Surgery,
Technische Universität München, Klinikum rechts der Isar,
Ismaningerstraße 22, 81675 Munich, Germany
Tel.: +49-89-41402171
Fax: +49-89-41406013
E-mail: R.Giunta@lrz.tu-muenchen.de

doi: 10.1111/j.1582-4934.2008.00592.x

ischemia and peripheral arterial disease [2–9]. In the field of reconstructive surgery we consider VEGF gene therapy pre-treatment of local flaps to increase flap dimensions the most promising application at this time. We were able to increase the length-to-width ratio in a random-pattern-flap model in the rats from 2:1 to 3:1 using an adenovirus encoding $VEGF_{165}$ [1]. The surviving flap size could be increased by 50% when gene therapy was performed 7 days prior to surgery. Despite these encouraging results, the use of an adenoviral vector hinders a clinical deployment.

One promising alternative to adenoviral vectors appeared to be the technique of magnetofection. The association of gene vectors with superparamagnetic nanoparticles and gene delivery under a magnetic field can boost the efficiency of many vector types up to several hundred-fold and this technique is available for most gene vectors [10]. The concentration of the vector in the target area and accumulation can both be enhanced by magnetofection methods [11]. In addition, magnetofection results in an enhanced dose–response relationship with a smaller amount of DNA required for sufficient gene expression [12].

The latest modification represents the combination of magnetic drug targeting and microsphere technology [13, 14]. Clinically, microspheres (or microbubbles) are applied as ultrasound contrast agents and experimentally as drug carriers and gene vectors [13, 15]. In this context, ultrasound is used to trigger an oscillation of bubble walls that eventually can lead to violent bubble burst, drug release and tissue perforation. Using microbubbles as drug carriers and using ultrasound for bubble burst has been demonstrated to be a powerful technique for localized delivery. Magnetic drug targeting and magnetofection are also tools for localized delivery. Therefore, we combined the two techniques by preparing acoustically active magnetic lipospheres that contain, apart from plasmid DNA, a high load of magnetic nanoparticles in the bubble shell. With these magnetobubbles, localized delivery, transgene release and cell penetration under a magnetic field is achieved by local application of ultrasound, leading to magnetobubble disruption [14]. In this study, we used acoustically active magnetic lipospheres containing the $VEGF_{165}$ cDNA in a lipid shell. We investigated the potential of magnetofection of the $VEGF_{165}$ gene on the survival and perfusion of the well-established oversized random-pattern-flap model in the rats [1, 16, 17] and compared the results to our previous findings using an adenoviral vector construct [1]. We evaluated the method with respect to the significance of applied magnetic field and ultrasound. Additionally we assessed VEGF-protein concentration in target tissue and analysed microvessel density and vessel diameter.

Material and methods

Magnetic lipospheres (magnetobubbles)

The plasmid pVF1164 encoding human $VEGF_{165}$ under the control of the CMV promoter was kindly provided by Dr. Michael Coleman (Valentis, Inc., previously The Woodlands, TX, USA). The plasmid pcDNA3.1$^{(+)}$EGFP encoding enhanced green fluorescent protein driven under CMV-promoter was kindly provided by Dr. Martina Anton (Institute of Experimental Oncology, Technische Universität München, Germany).

Both plasmids were kept as stock solutions in deionized water. Iron oxide nanoparticles coated with Tween 60 (fluidMAG-Tween 60; 90 mg/ml in water) were kindly provided by Christian Bergemann (chemicell GmbH, Berlin, Germany). The cationic lipid being the major component of the cationic lipid transfection reagent Metafectene™ was kindly provided by Dr. Stephan König (Biontex GmbH, Martinsried, Germany). 1,2-dioleoyl-*sn*-glycero-3-phosphoethanolamine (DOPE) was purchased from Avanti Polar lipids (Alabaster, AL, USA). Soybean oil was provided by the hospital pharmacy at the authors' institution.

Preparation of magnetobubbles

For magnetic lipospheres preparation (MAAL: Tw60-Mag/pDNA), a lipid stock solution containing Metafectene (1.06 mM) and DOPE (3.6 mM) was prepared in buffer (NaCl 0.9%: glycerol: propylene glycol in 8:1:1 v/v). In a microcentrifuge tube, magnetic nanoparticles coated with Tween 60 (fluidMAG-Tween 60, with nanomaterial concentration of 90 mg/ml) (11.1 μl) were mixed with the lipid stock solution (90.5 μl). These core-shell particles have a hydrodynamic diameter of 150 nm as determined by dynamic light scattering and a maghemite core (from gamma Fe_2O_3) of 10 nm. The ζ-potential lies at -8.9 ± 1.0 mV (in 0.9% NaCl). The theoretical (mathematical) number of particles is calculated ~5.19×10^{14}/g nanomaterial with a density of ~1.25 g/cm^3. The mixture was diluted to 858 μl with buffer. Plasmid DNA (*e.g.* pBluc) (40 μl of a 1 mg/ml plasmid dilution) was added to the mixture and mixed well. The mixture was pipetted in a 2-ml Wheaton vial (Wheaton, Millville, NJ, USA), where soy bean oil (5% v/v) was already pipetted, and sealed with an aluminium sealing cup with a rubber liner (13 mm E-Z seal aluminium natural w/red natural rubber liner / Wheaton, Millville, NJ, USA). Using a three-needle stopcock (Braun, Melsungen, Germany), perfluoropropane gas (C_3F_8) (Linde AG, Höllriegelskreuth, Germany) filled the headspace of the vial. The vial was shaken for 60 sec., at 2500 rpm using a Mini BeadBeater (Biospec Products Inc., Bartlesville, OK, USA).

Size and concentration of lipospheres were determined using a Coulter Counter. The size of prepared magnetobubbles mainly lies in the range of 2–4 μm, with a mean diameter of 1.98 μm, median and mode of 1.78 μm and 1.43 μm, respectively. A 4% of magnetic microbubbles lie in the range of 4–10 μm with a mean diameter of 6.1 μm, median and mode of 5.88 μm and 4.30 μm, respectively. Visual observation of the magnetobubbles suspension did not lead to the conclusion that the microbubbles are interconnected, something that one might have expected due to the presence of the magnetic particles (Figs 1 and 2).

The incorporation of plasmid DNA was verified in independent magnetobubble preparations using 125-iodine labelled plasmid DNA and gamma counting of supernatants upon magnetic sedimentations or of subnatants after bubble flotation. The incorporation efficiency of plasmid DNA with the chosen ratios of bubble components was almost quantitative (94% of the DNA dose was associated with magnetic microbubbles). Similarly, magnetic nanoparticle incorporation into the liposheres was almost quantitative as determined by photometric turbidity measurements at 630 nm.

pDNA release upon insonication was measured after preparation of magnetobubbles loaded with an amount of J^{125}labelled pDNA (8×10^5 cpm/ml magnetobubbles) and complemented upon 40 μg with non-labelled pDNA. The amount of radioactive pDNA was 27% of the total plasmid loaded on the magnetobubbles. In a 24-cell culture plate filled

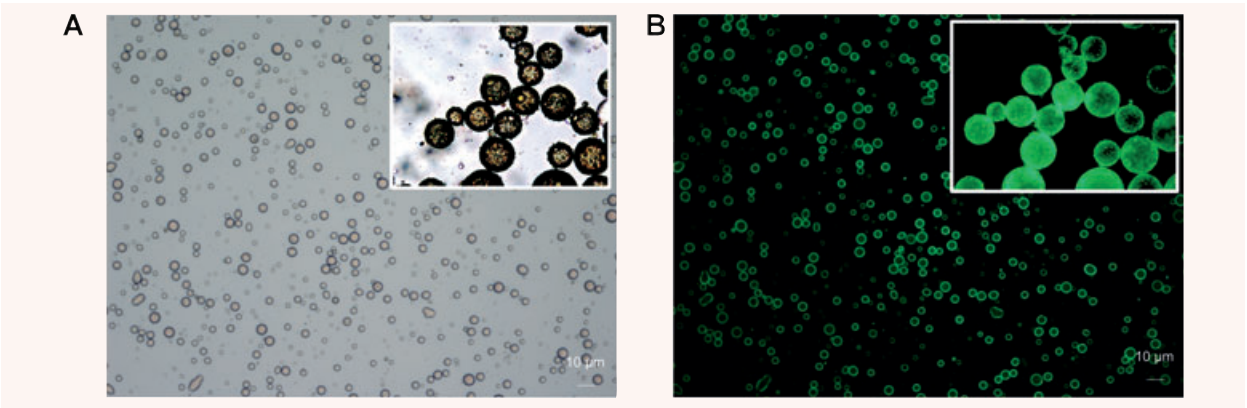

Fig. 1 (**A** and **B**) Magnetobubbles 1(a) Acoustically active magnetic lipospheres (magnetobubbles) containing a high load of magnetic nanoparticles (black) in the bubble shell as pictured in phase contrast microscopic images. The size of prepared magnetobubbles mainly lies in the range of 2–4 μm, with a mean diameter of 1.98 μm. 2(b) Visualization of plasmids in pBLuc labelled with YOYO-1 (excitation 390 nm/ emission 460 nm; Molecular Probes, Eugene, OR, USA).

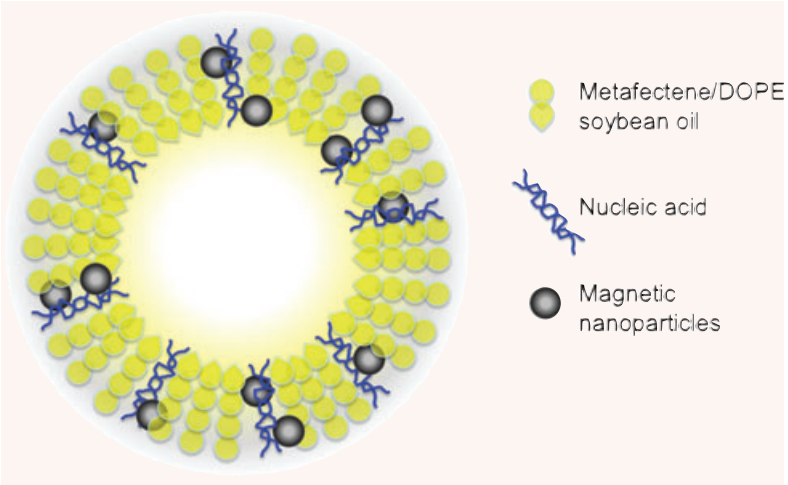

Fig. 2 Configuration of magnetobubbles. Suggested configuration of acoustically active magnetic lipospheres (magnetobubbles), modified from Unger *et al.* and Vlaskou *et al.*

with 2 ml ddH_2O 50 μl (~4 × 10^4 cpm) of radioactive magnetobubbles was added. The cell culture plate was put on a magnetic plate (neodymium–iron–boron permanent magnets attached to a galvanized iron plate, OZ Biosciences, France) for 10–15 min. The magnetic field applied was 1080–1150 mT with gradient of the field of >50 T/m. Ultrasound (Sonitron 2000D ultrasound device operating at 1 MHz (Rich Mar Inc., Inola, OK, USA) with power intensity of 4 W/cm^2 at 50% or 100% duty cycle was applied using a 6-mm ultrasound probe of SONITRON 2000D (as *in vivo* applications) for different time periods. The cell culture plate remained on magnetic plate for 10–15 min. and subsequently the radioactivity of 1 ml of supernatant was measured with a WALLAC γ-counter (Wallac 1480 Wizard 3', PerkinElmer Wallac, Freiburg, Germany).

For the evaluation of the ultrasound influence in *in vitro* applications (experiments), the same experiment was carried out in 96-cell culture plate filled with 250 μl ddH_2O and with the addition of 50 μl (~4 × 10^4 cpm) of radioactive magnetobubbles [18]. Magnetic field of 130–240 mT and gradient of the field of 70–120 T/m was applied using 96-Magnets Magnetic Plate (OZ Biosciences, France). Ultrasound was applied with a power intensity of 1, 1.5 and 2 W/cm^2, with 50% or 100% duty cycle at a frequency of 1 MHz using a 3-mm ultrasound probe of SONITRON 2000D (as *in vitro* applications) for different time periods. The radioactivity of 150 μl of supernatant was measured with a WALLAC γ-counter.

Magnetic applicator characteristics

The magnetic field was applied using a magnetic applicator composed of six NeFeB disk magnets (d = 20 mm, h = 5 mm) and three steel cylinders (d = 20 mm, h = 120 mm) (Fig. 3). The magnetic induction z-component values B_z were measured in a 1-mm grid in a plane (x, y) parallel to and at different distances z from the working surface of the applicator and used to calculate z-component of a magnetic field gradient in z-direction dB/dz. In a 'working area' up to 2–3 mm over the surface of the applicator

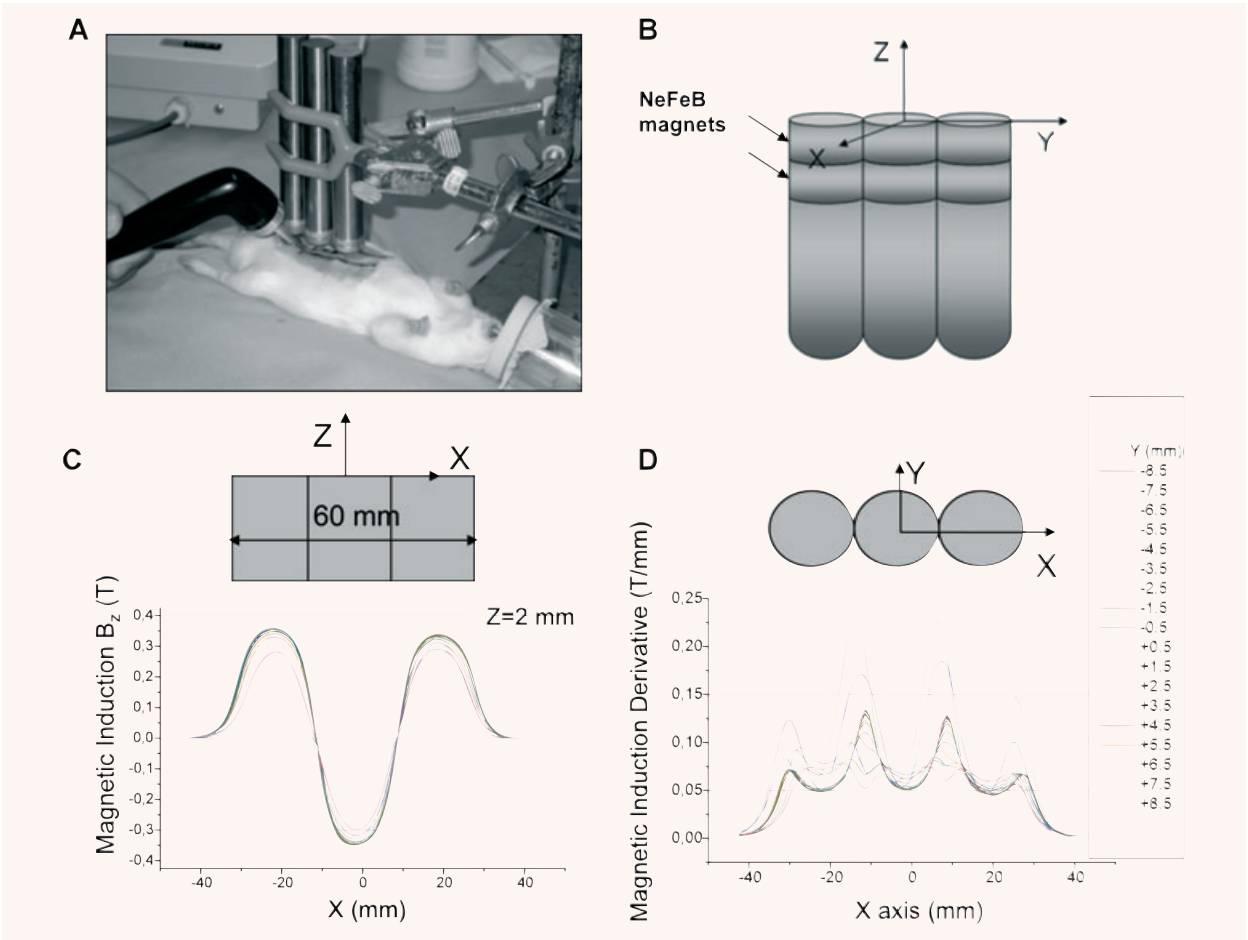

Fig. 3 (**A**–**D**) Experimental set-up (**a**) and magnetic applicator characteristics (**b**–**d**). The magnetic field was applied using a magnetic applicator composed of six NeFeB disk magnets ($d = 20$ mm, $h = 5$ mm) and three steel cylinders ($d = 20$ mm, $h = 120$ mm) as shown in a photo ***a*** and scheme ***b***. The magnetic induction *z*-component values B_z were measured in a 1 mm grid in a plane (*x*, *y*) parallel to and at different distances *z* from the working surface of the applicator and used to calculate *z*-component of a magnetic field gradient in *z*-direction dB/dz (shown in graphs ***c*** and ***d*** for $z = 2$ mm). In a 'working area' up to 2–3 mm over the surface of the applicator magnetic field induction and its derivative were found to be predominantly higher than 0.2 T and 0.05 T/mm, respectively.

magnetic field induction and its derivative were found to be predominantly higher than 0.2 T and 0.05 T/mm, respectively.

Study design and animal experiments

Forty-six male Sprague-Dawley rats with an average weight of 350 g were used in this study. Animals were caged individually and standard laboratory food for rats and water was provided *ad libitum*. The procedures involving animal treatment and care were conducted in conformity with the institutional guidelines that are in compliance with national and international laws and policies (EEC council directive 86/609, OJ L 358, 1, December 12, 1987; NIH guide for the care and use of laboratory animals, NIH publication no. 85-23, 1985).

All surgical procedures were performed under standard aseptic conditions. In all experiments anaesthesia was induced and maintained by spontaneous inhalation of isofluran and oxygen.

Design of skin flap

A rectangular skin flap with a cranial pedicle was outlined on the right abdominal wall. The medial margin ran from the xiphoid process, 8 cm caudally. The lateral margin was 2 cm lateral from and parallel to the medial margin forming the 2×8 cm flap. This flap design is well established and produces a consistent necrosis of the distal half due to the flaps extended dimension [1, 16, 19, 20]. Perfusion of the abdominal region of the rat is similar to that of the human and thus this model can be modified to simulate perforator-flaps (DIEP-flap) and musculocutaneous flaps (TRAM).

Table 1 Study design

Group	Therapy	Evaluation
A1 ($n = 6$)	VEGF-bubbles + magnet + ultrasound; 7 days pre-OP	Measurement of flap size, indocyanine green (ICG) laser-fluoroscopy; 7 days post-OP
A2 ($n = 6$)	VEGF-bubbles + magnet; 7 days pre-OP	Measurement of flap size, ICG laser-fluoroscopy; 7 days post-OP
A3 ($n = 6$)	VEGF-bubbles + ultrasound ; 7 days pre-OP	Measurement of flap size, ICG laser-fluoroscopy; 7 days post-OP
A4 ($n = 6$)	− Controls − GFP-bubbles + magnet + ultrasound ; 7 days pre-OP	Measurement of flap size, ICG laser-fluoroscopy; 7 days post-OP
A5 ($n = 6$)	− Controls − NaCl 7 days pre-OP	Measurement of flap size, ICG laser-fluoroscopy; 7 days post-OP
P1 ($n = 6$)	VEGF-bubbles + magnet + ultrasound 7 days pre-OP	VEGF-ELISA; 7 days after therapy
P2 ($n = 6$)	− Controls − NaCl 7 days pre-OP	VEGF-ELISA; 7 days after therapy
D1 ($n = 2$)	VEGF-bubbles + magnet + ultrasound 7 days pre-OP	Assessment of microvessel density, assessment of vessel diameter; 7 days after therapy
D2 ($n = 2$)	− Controls − NaCl 7 days pre-OP	Assessment of microvessel density, assessment of vessel diameter; 7 days after therapy

Experimental and control groups and associated therapy and techniques of evaluation.

Magnetobubble injection

The treatment (magnetobubble magnetofection of the $VEGF_{165}$ gene or controls) was carried out 7 days before surgery (Table 1). This interval between gene therapy and surgery yielded best results in our previous angiogenesis research [1]. Prior to injection of vectors, the abdominal skin was shaved under anaesthesia from sternum to the pubic region. In groups A1–A3, P1 and D1 a total of 200 μl volume of magnetobubbles containing $VEGF_{165}$ cDNA was injected subcutaneously in four aliquots of 50 μl each into the distal half of the overdimensioned future flap (Fig. 4A). Injection sites are placed centrally in the distal half with a distance of 1 cm to another. The distal half of the future skin flap will be critically perfused once the flap is raised and thus serves as our region of interest. Here the tissue will benefit from an optimized vascular network. Quantification of magnetobubbles using a Coulter counter indicated that about 2×10^9 magnetobubbles formed per millilitre of suspension. An injection of 200 μl of suspension results in a number of 0.5×10^9 magnetobubbles loaded with 8 μg pDNA (VEGF).

Hereafter a magnetic field (IBS magnet, Berlin, Germany; Al–Ni–Co rod magnet 120 × 20 mm, provided at its end with two additional Nd–Fe–B disk magnets 20 × 5 mm, NeoDelta magnet #NE205) was applied for 15 min. (groups A1, A2, A4, P1, D1) over the injection sites (Fig. 4B). This incubation time was found to be sufficient for a successful transfection [12]. In the 'working area' 2–3 mm below the surface of the applicator magnetic induction and its derivative are predominantly >0.2 T and >50 T/m, respectively. After 5 min. under the magnetic field, ultrasound was applied additionally (groups A1, A3, A4, P1, D1) for a total of 5 min. to the four injection spots (Fig. 4C), followed by another 5 min. of magnetic force alone. For insonication, a Sonitron 2000 sonoporator was used (Rich-Mar, Inola, OK, USA; 6 mm probe, 4 W/cm^2 and 100% duty cycle at a frequency of 1 MHz). In order to test the contribution of ultrasound and magnetic force to the therapeutic effect, we also tested the administration of the magnetic force (group A2) and ultrasound alone (group A3). Administration of magnetic microbubbles containing GFP cDNA (group A4) and saline injection (groups A5, P2, D2) served as controls.

In groups A1–A5 surgery was scheduled 7 days after therapy. Postoperatively, flap perfusion was measured using indocyanine green (ICG-) laser-fluoroscopy.

In groups P1 and P2 protein concentration in treated skin and underlying muscle was assessed 7 days after therapy by means of ELISA.

In groups D1 and D2 microvessel density and vessel diameters were analyzed on day 7.

Surgical technique

Surgery was scheduled 7 days after microbubble administration.

After depilation of the anterior abdominal wall and marking of the flap design, the flap was raised in the subcutaneous layer between skin and muscle. All perforating vessels reaching the skin from the inferior and superior epigastric artery were carefully divided. After haemostasis was obtained, the flap was repositioned and sutured back into place with interrupted sutures.

$VEGF_{165}$ ELISA

In groups P1 and P2 (control) the skin flaps and underlying muscle were harvested 7 days after magnetobubble administration and immediately shock-frozen in liquid nitrogen. Both skin and muscle specimens were divided into the proximal and distal halves in analogy to the flap design with the distal half being critically perfused and bearing the injection sites.

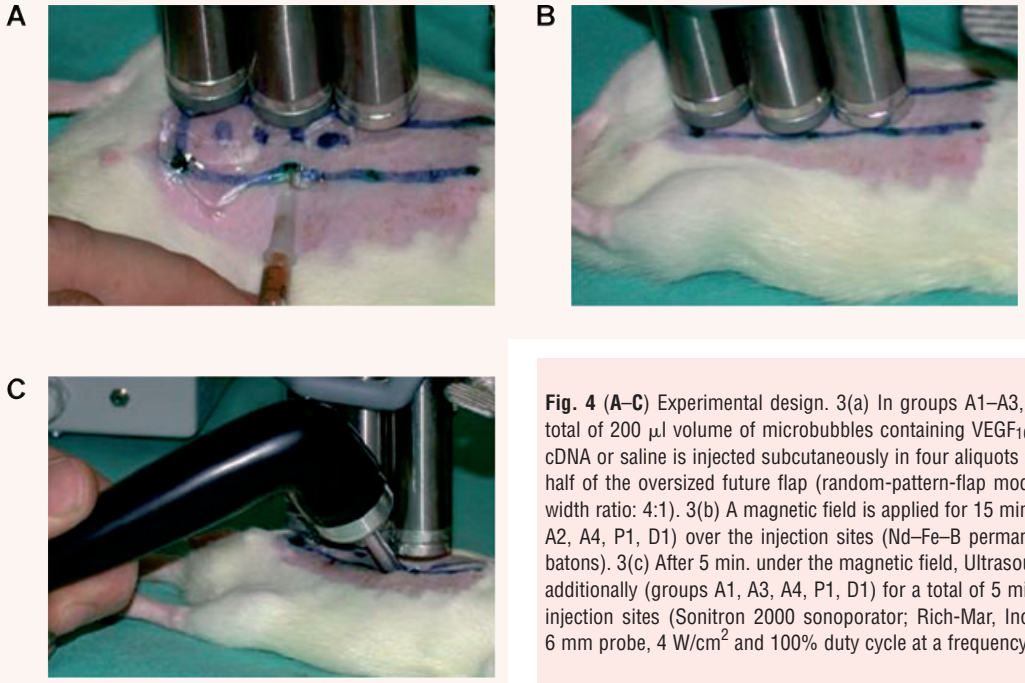

Fig. 4 (**A–C**) Experimental design. 3(a) In groups A1–A3, P1 and D1 a total of 200 μl volume of microbubbles containing $VEGF_{165}$ cDNA, GFP cDNA or saline is injected subcutaneously in four aliquots into the distal half of the oversized future flap (random-pattern-flap model; length-to-width ratio: 4:1). 3(b) A magnetic field is applied for 15 min. (groups A1, A2, A4, P1, D1) over the injection sites (Nd–Fe–B permanent magnetic batons). 3(c) After 5 min. under the magnetic field, Ultrasound is applied additionally (groups A1, A3, A4, P1, D1) for a total of 5 min. to the four injection sites (Sonitron 2000 sonoporator; Rich-Mar, Inola, OK, USA; 6 mm probe, 4 W/cm^2 and 100% duty cycle at a frequency of 1 MHz).

Underlying muscle was removed to analyse whether or not the effect was limited to the treated skin.

Tissue samples were homogenized with 250 μl of zirconia / silica beads (Biospec, Bartlesville, OK, USA) and 250 μl lysis buffer (Reporter lysis buffer, Qiagen, Hilden, Germany) at 4200 rpm for a total of 40 sec. (1×20 sec. $+ 2 \times 10$ sec.) using the Mini-BeadBeater-1™ (Biospec Products, Bartlesville, OK, USA). The homogenate was subsequently centrifuged for 15 min. at 21,000 $\times$ *g* at 4°C. The supernatant was separated in aliquots and kept frozen until analysis using a quantitative sandwich enzyme immunoassay (RayBio® Human VEGF ELISA Kit, RayBiotech Inc., Norcross, GA, USA).

Supernatants were thawed, particulars were removed by centrifugation and the samples were diluted 1:2 and added to the kit. Upon completion of the assay procedure standard and samples were read at 450 and 550 nm λ-correction.

Indocyanine green laser-fluoroscopy

ICG (Pulsion Medical Systems AG, Munich, Germany) is a tricarbocyanine dye that binds almost completely to globulins and is exclusively distributed in the intravascular space. ICG has a normal plasma half-life of 3 to 4 min., is not metabolized in the body and is eliminated exclusively through the liver and excreted into the bile. ICG-fluorescence was induced and recorded using a laser-fluorescence imaging device (IC-View®, Pulsion Medical Systems AG), comprising a NIR laser light source (0.16 W, wavelength λ 780 nm) and a NIR-filtered digital camcorder. In groups A1–A5, a bolus of 0.3 mg/kg bodyweight was injected directly after surgery into a tail vein under general anaesthesia [16, 17]. The fluorescence was recorded with a digital camera and the grey scale images transferred to an image analysing system (IC-Calc®, Pulsion Medical Systems AG).

According to flap design, the distal half was critically perfused and therefore evaluated as the region of interest. The perfusion index (increase of grey value/time) was recorded in relation to the surrounding skin with normal blood flow. A standard provided exclusion of artefacts due to automatic adaptation of the camera's shutter.

Measurement of flap size

In groups A1–A5, digital images were taken perpendicular to the flap 7 days after surgery. Pictures were analysed using NIH Image Software (National Institutes of Health, MD, USA).

Microvessel density

Flap microvessel density was assessed in skin and underlying muscle using a monoclonal CD31 antibody (Serotec, mouse antirat, MCA 1334G) in groups D1 and D2 (control) 7 days after magnetobubble administration. Along the borders of the projected flap the anterior body wall was harvested after killing the animals. The skin was separated along the fascia from the underlying muscle. From each portion of flap and muscle (proximal and distal halves), three skin and three muscle samples were isolated and frozen in liquid nitrogen. After cryosectioning and incubation with the antibody, haematoxylin was used for nuclear counterstaining. From each specimen three representative images with a primary magnification of ×100 were taken with an Axiophot photomicroscope (Carl Zeiss, Oberkochen, Germany) and downloaded into a morphometry and image analysis program (Diskus 4.50.20, Hilgers, Königswinter, Germany).

Microvessel density was determined with a modified 25-point Chalkley graticule [21, 22], a validated, rapid and reproducible method for clinical

research use. The Chalkley grid was superimposed on the TFT display of the image analysis program. With the final magnification of 345×, the Chalkley grid had a diameter of 350 μm. The grid was orientated so that the maximum number of points possible overlapped highlighted vessels.

Vessel diameter

Vessel diameter and morphometry were assessed by means of corrosion casting [23, 24]. In animals of groups D1 and D2, the aorta was cannulated with an olive-tipped cannula (Acufirm, Dreieich, Germany) after thoracotomy under intraperitoneal anaesthesia and systemic heparinization 7 days after surgery. Then body temperature saline was infused to rinse the vascular system. Vessels were fixed by infusion of body temperature glutaraldehyde solution (2.5% phosphate-buffered glutaraldehyde, pH 7.4). Thereafter the systemic circulation was perfused with Mercox™ (SPI, West Chester, PA, USA) mixed with 4:1 diluted methylmetacrylate monomers (Aldrich Chemicals, Milwaukee, WI, USA) over a period of 2–5 min. After polymerization, the presumptive flap along with the underlying portion of the rectus muscle was raised and macerated in 5% potassium hydroxide followed by drying and mounting for scanning electron microscopy. Having coated the casts with gold in an argon atmosphere, the corrosion casts were imaged using a scanning electron microscope (ESEM XL30, Philips, Eindhoven, Netherlands). Stereo-pair images were obtained using a tilt angle of 6° [24]. After digital storage of calculated images diameters were measured orthogonal to the vessel axis using v2.1 AnalySIS® software. Intervessel distances were quantified in stereo-pairs using KS300® software (Kontron, Eching, Germany).

Statistical evaluation

Statistical evaluation between groups was performed using the non-parametric Kruskal–Wallis and Mann-Whitney tests; $P < 0.05$ was considered statistically significant. Multiple testing was taken in account according to the method of Marcus *et al.* [25].

Results are presented in box-plots with the box representing the interquartile range and the line within the box being the median. Vertical lines represent the adjacent values.

Results

$VEGF_{165}$ ELISA

VEGF expression in skin flaps showed enhanced VEGF concentration after magnetobubble magnetofection compared to controls. The underlying rectus abdominis muscle was investigated to determine whether the effect is restricted to the treated skin.

Seven days after therapy we measured a significant increase in VEGF-protein concentration in the target tissue (distal half of skin flaps):

We measured an average VEGF concentration of 520 pg/g (SD: 130 pg) tissue in the treated distal halves of the skin flaps in group P1 (VEGF-bubbles + magnet + ultrasound) and 471 pg/g (SD: 60 pg) tissue in the proximal halves.

In controls (group P2), we measured an average VEGF concentration of 145 pg/g (SD: 31 pg) tissue in the distal half of the skin flaps and 150 pg/ng (SD: 16 pg) tissue in the proximal half. Differences between P1 and P2 were statistically significant ($P < 0.05$) (Fig. 5A and B).

The VEGF protein concentration in the underlying muscle did not differ statistically significant ($P > 0.05$), thus indicating a locally restricted effect of the therapy (Fig. 6A and B). In group P1 an average concentration of 169 pg/g tissue was found in the proximal half of the muscle and an average of 90 pg/g tissue in the distal halves. Controls (group P2) showed an average concentration of 110 pg/g tissue in the proximal half of the muscle and an average of 121 pg/g tissue in the distal halves.

Indocyanine green laser-fluoroscopy

Flap perfusion was measured post-operatively in groups A1–A5 by means of perfusion index (ratio of arterial inflow / time) in the distal – and thus by definition critically perfused – halves of the flaps.

In group A1 (VEGF magnetofection, magnet + ultrasound), we measured an average perfusion index of 39% compared to regularly perfused surrounding tissue.

Group A2 (VEGF magnetofection, magnet alone) presented an average index of 26% and group A3 (ultrasound alone) an average index of 28%.

GFP controls (group A4, GFP magnetofection) and saline controls (group A5) showed indices of 23% and 21% respectively.

Differences between groups A2–A5 were statistically not significant ($P > 0.05$), whereas group A1 presented a significantly increased perfusion index when compared to all other groups ($P < 0.05$) (Fig. 7).

Measurement of flap size

In group A1 (VEGF magnetofection, magnet + ultrasound) flaps showed an average necrosis of only 25.7% of total flap size on day 7 after surgery (surviving area: 8.93 cm^2; necrosis: 3.09 cm^2).

In group A2 (VEGF magnetofection, magnet alone) an average necrosis of 36.8% could be recorded (surviving area: 7.52 cm^2; necrosis: 4.31 cm^2).

Group A3 (VEGF magnetofection, ultrasound alone) demonstrated an average necrosis of 44.5% of total flap size (surviving area: 5.8 cm^2; necrosis: 4.43 cm^2).

In GFP controls (group A4; GFP magnetofection) an average of 50.8% of total flap size was recorded necrotic (surviving area: 5.77 cm^2; necrosis: 5.82 cm^2) and saline controls (group A5) showed an average flap necrosis of 49.86% (surviving area: 4.1 cm^2; necrosis: 4.08 cm^2).

Group A1 (presented a statistically significant reduction of flap necrosis when compared to all other groups ($P < 0.05$). Only the combination of a magnetic field and the application of ultrasound after VEGF-microbubble magnetofection led to a

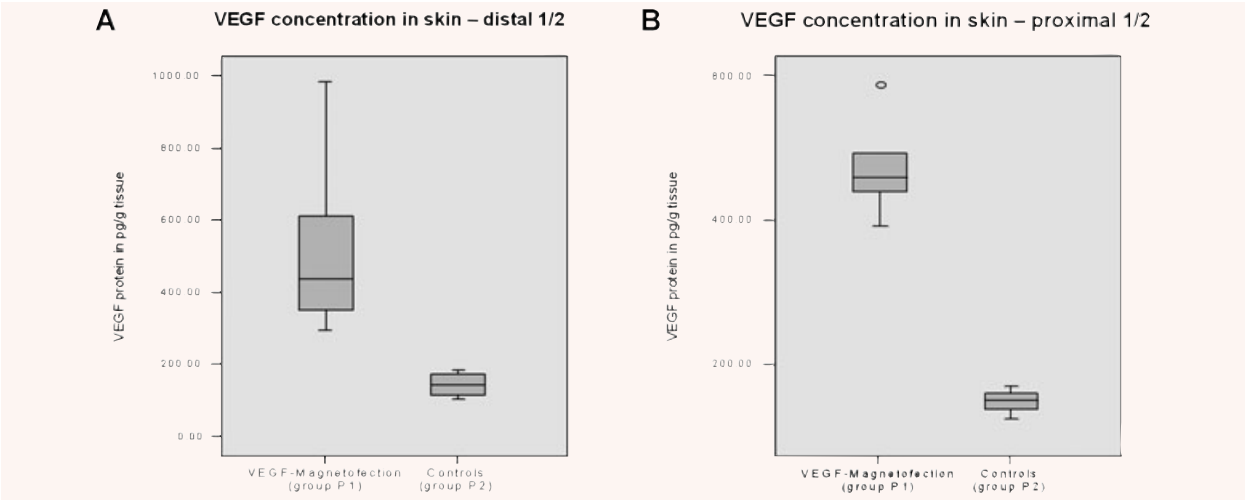

Fig. 5 (**A** and **B**) VEGF concentration in skin. VEGF expression in skin flaps showed significantly enhanced ($P < 0.05$) VEGF concentration after magnetobubble magnetofection (group P1; VEGF magnetofection, magnet + ultrasound) compared to controls (group P2, NaCl 0.9%). Injection sites were localized in the distal ½ of the flaps.

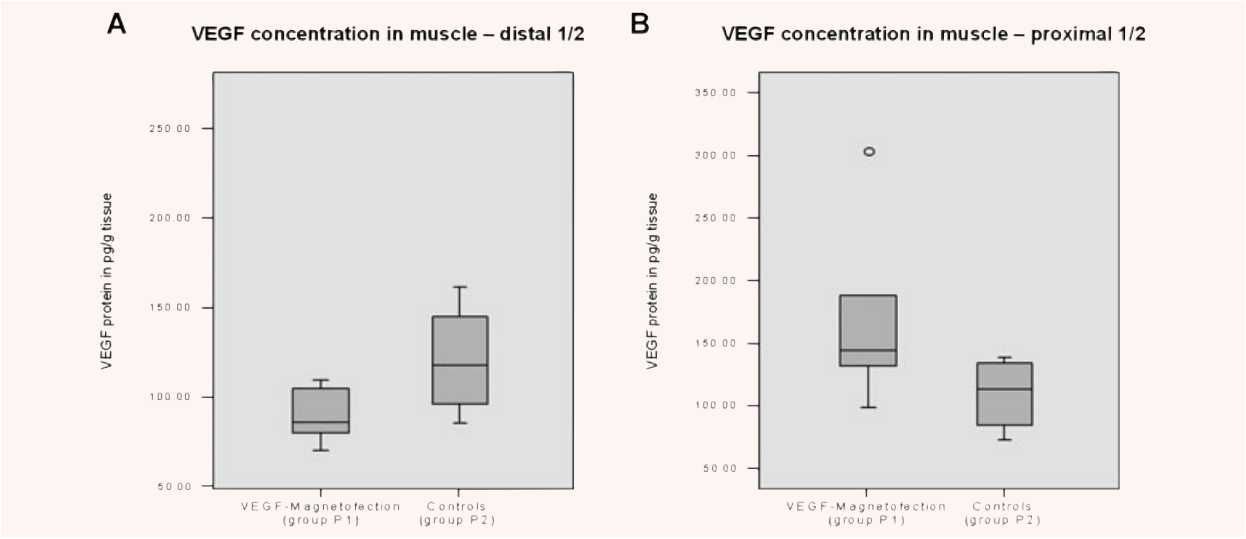

Fig. 6 (**A** and **B**) VEGF concentration in muscle. VEGF protein concentration in the underlying muscle did not differ statistically significant ($P > 0.05$), thus indicating a locally restricted effect of the therapy.

significant increase in flap survival and reduction of necrosis (Figs. 8A and B, 9).

Microvessel density

An average of 7.2 Chalkley points could be counted in the sub-follicular subcutical layer of the distal halves of flaps of group D1 (VEGF magnetofection, magnet + ultrasound), whereas controls (group D2; NaCl 0.9%) averaged 6.2 Chalkley points.

In the parafollicular subcutical layer of the distal halves of the flaps quantitative morphometry resulted in 4.0 Chalkley points for group D1 and 4.1 for controls (group D2) on average.

Figure 10A creates an impression of increased microvessel density, but differences in both layers were statistically not significant ($P > 0.05$) (Fig. 10B).

The vessel densities in the underlying musculature were also not affected ($P > 0.05$) by the treatment (4.3 Chalkley points in group D1, 4.0 Chalkley points in group D2 on average).

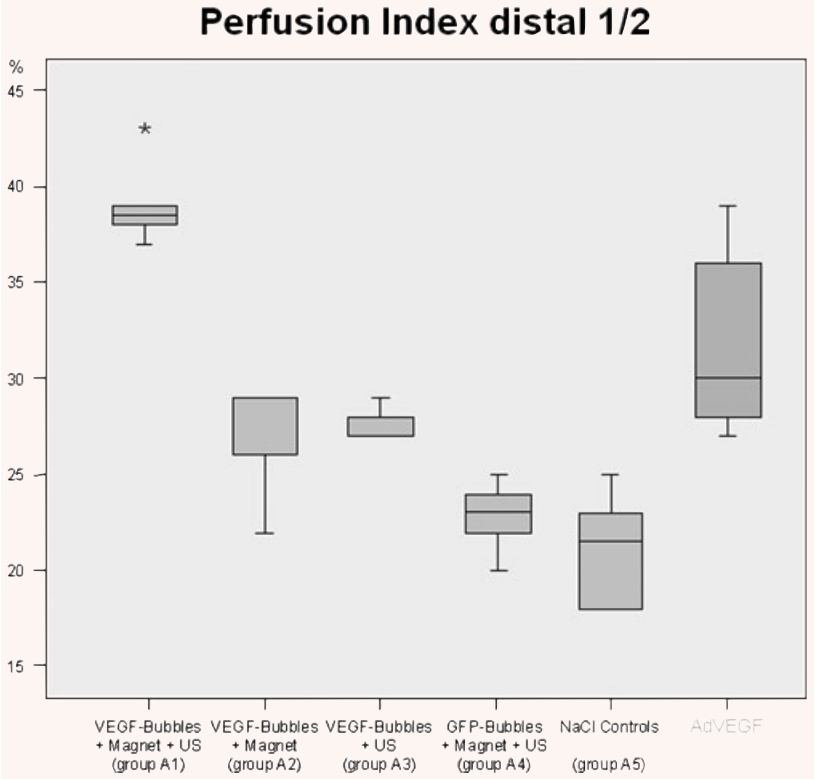

Fig. 7 Flap perfusion. Flap perfusion was measured post-operatively in groups A1–A5 by means of perfusion index (ratio of arterial inflow / time) in the distal half of the flaps. Differences between groups A2–A5 were statistically not significant ($P > 0.05$), whereas group A1 (VEGF magnetofection, magnet + ultrasound) presented a significantly increased perfusion index when compared to all other groups ($P < 0.05$). Results compared to adenoviral transduction of 5×10^8 pfU $VEGF_{165}$ on the right [1].

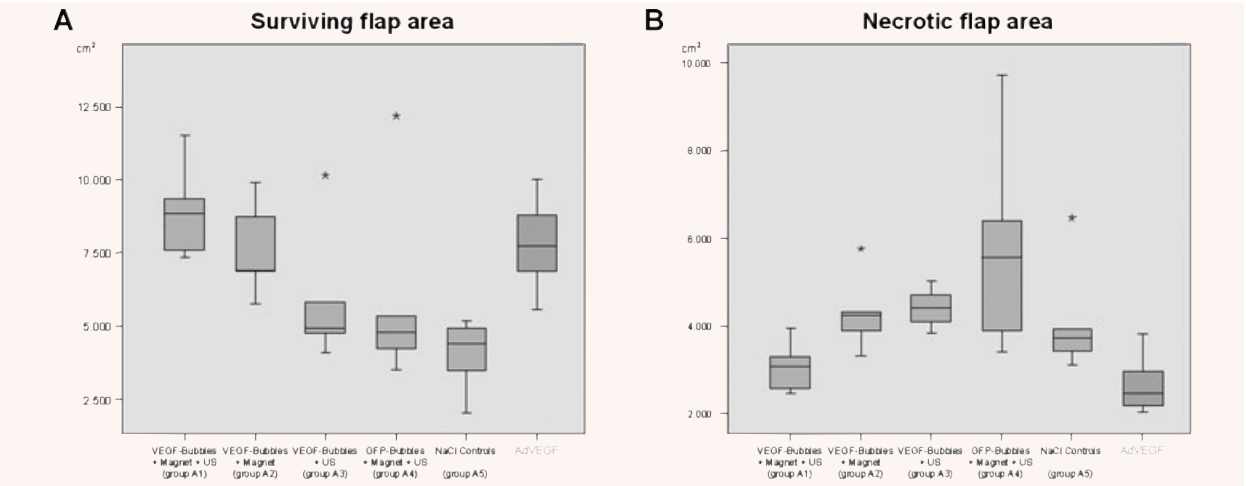

Fig. 8 (**A** and **B**) Surviving and necrotic flap areas. Group A1 A1 (VEGF magnetofection, magnet + ultrasound) presented a statistically significant reduction of flap necrosis when compared to all other groups ($P < 0.05$). Only the combination of a magnetic field and the application of ultrasound after VEGF-microbubble magnetofection (group A1) led to a significant increase in flap survival and reduction of necrosis. Results compared to adenoviral transduction of 5×10^8 pfU $VEGF_{165}$ on the right [1].

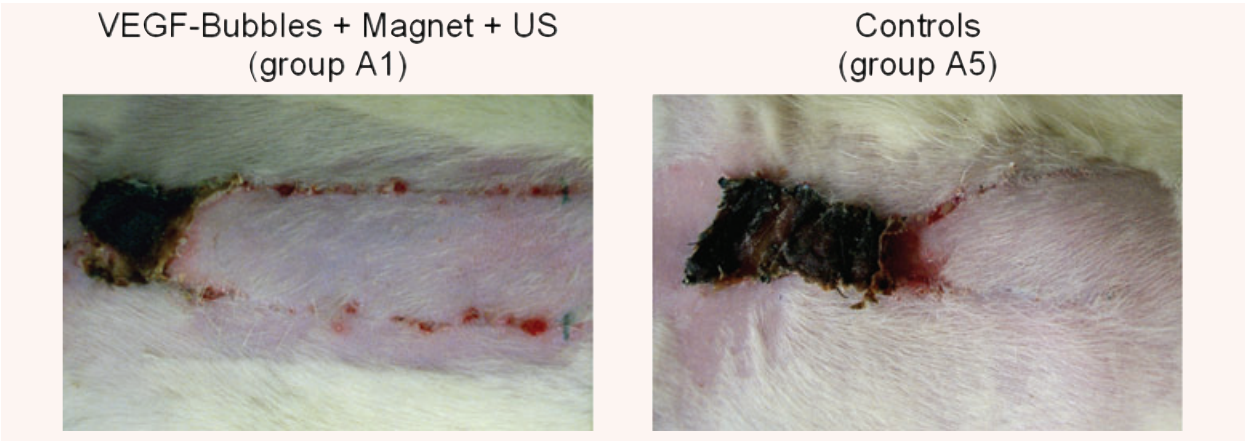

Fig. 9 Results at day 7. Flap appearance 7 days after surgery. A statistically significant reduction of flap necrosis was seen in group A1 (VEGF magnetofection, magnet + ultrasound), here opposed to saline-controls on the right (group A5).

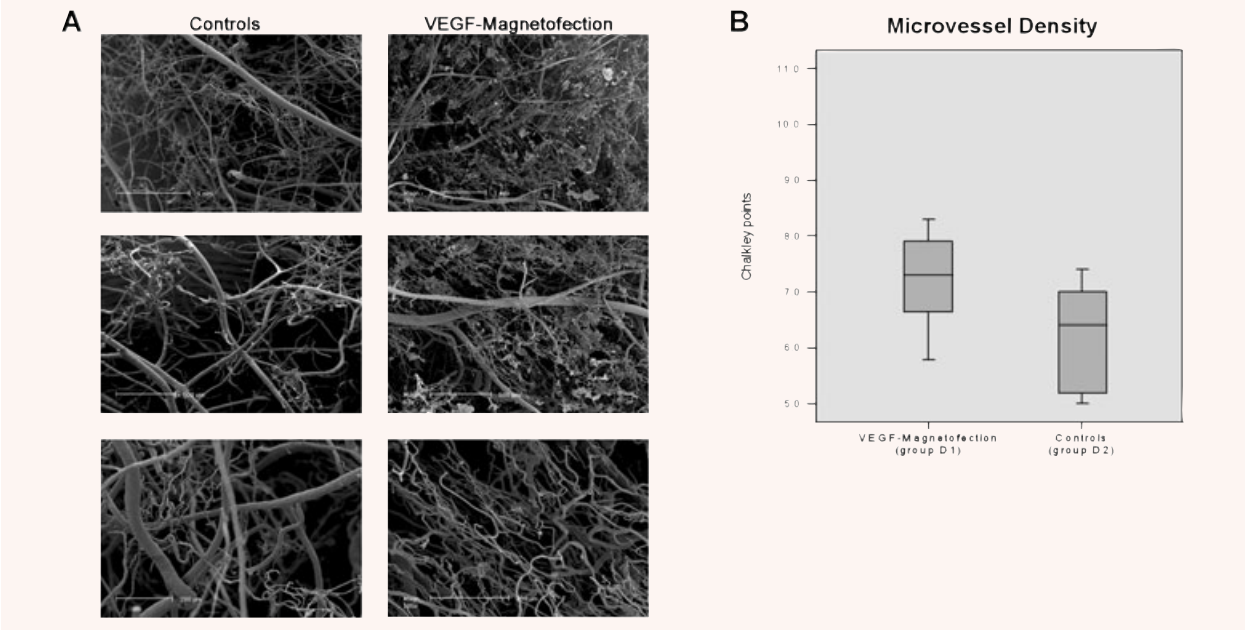

Fig. 10 (**A** and **B**) Microvessel density. Vessel diameter and morphometry were assessed by means of corrosion casting 7 days after VEGF-microbubble magnetofection (group D1) and in controls (group D2; NaCl 0.9%). Differences were statistically not significant ($P > 0.05$).

Vessel diameter

Vessel diameter and morphometry were assessed by means of corrosion casting 7 days after VEGF-microbubble magnetofection (group D1) and in controls (group D2) (Fig. 10A).

An average vessel diameter of 5.7 μm could be recorded, whereas in control animals the diameter measured 7.2 μm on average. Differences were statistically not significant ($P > 0.05$).

Discussion

Magnetofection of the $VEGF_{165}$ gene using acoustically active magnetic lipospheres led to an increased VEGF protein concentration in the target tissue, induced an enhanced blood flow and resulted in a reduced rate of necrosis in this setting. The findings of this study further elucidate the contribution of both magnetic force and ultrasound to the effect of magnetobubble magnetofection.

It turned out that only the combination of both resulted in significantly improved results.

Increased VEGF expression was restricted to the target tissue, the underlying rectus muscle showed no effect. Nonetheless, magnetobubble magnetofection of $VEGF_{165}$ did not result in a commensurable higher density of microvessels. The average Chalkley count was higher than in controls, but failed to reach statistical significance. This is in agreement with reports from other authors who also did not find an increased microvessel density despite significantly increased skin flap survival upon treatment with VEGF encoding naked plasmid DNA in a similar model [26]. Yet, the perspicuous increase in flap perfusion we measured 7 days after VEGF-magnetofection strongly suggests that localized VEGF overexpression resulted in angiogenesis. The factor VEGF is widely examined and its angiogenic potential is proven. The disadvantages of a VEGF monotherapy, such as formation of immature and leaky vessels or tissue oedema are known. With this knowledge a combination of VEGF with other growth factors, *e.g.* Angiopoietin1 or bFGF appears to be promising and is currently evaluated by our work group.

When compared to our previous work using adenoviral transduction of $VEGF_{165}$, magnetobubble magnetofection produced comparable results [1]. This finding is quite encouraging, given the fact that adenoviral vectors count among the most efficient gene vectors known. Both methods, adenoviral transduction and magnetofection of liposphere, resulted in a statistically significant increase of viable flap area (AdVEGF: 74.1%; microbubbles: 74.3%) and blood flow in the distal halves of the flaps (AdVEGF: 32%; microbubbles: 39%). These results confirm that an increased length-to-width ratio of 3:1 in random-pattern flaps is a realistic goal. This could have a clinical impact since indications for random-pattern-flaps may now overcome limitations due to flap size and arc of rotation – as well as all different kinds of flap models, ischemic skin or wound edges in general would also benefit from an improved tissue perfusion.

In this study, magnetic force alone did not significantly improve the biological effect. This result stands in analogy to Huth *et al.* [27], who demonstrated that magnetic force does not lead to a direct cellular uptake mechanism circumventing the endosomal pathway in cell culture experiments with standard magnetofection – in other words, that magnetic forces like used in our study are insufficient to force gene vectors through the plasma membrane into the cytoplasm. Interestingly, the use of ultrasound alone upon magnetobubble administration did not result in a statistically significant improved outcome in our experimental set-up, either. This was surprising because it is known that ultrasound can induce a significant increase in cutaneous blood flow [28], although this effect is transient. But based on the state of the art in gene delivery by sonoporation using ultrasound [29] and 'conventional' microbubbles we would definitely have expected a significant improvement of biological outcome over controls. This finding may be explained by the increased rigidity that the magnetobubbles used here display compared with conventional microbubbles (*e.g.* Optison). pDNA release upon insonation was demonstrated by loading of magnetobubles with J^{125}-labelled pDNA; our magnetobubbles require a much longer exposure to ultrasound and higher power to induce bubble burst than for example Optison (hence the long exposure time at high power used in our experiments). Moreover, due to our preparation method, plasmid DNA is likely an integral part of the bubble shell whereas in 'conventional' sonoporation the nucleic acid is usually bound to the surface of pre-formed microbubbles, which may facilitate cellular uptake upon ultrasound-induced bubble burst. In fact, the motivation for developing *magneto*bubbles instead of using conventional microbubbles was providing a carrier that is responsive to two independent physical forces and that 'delivers' only if the two forces are used in combination. The intended use is obviously combining magnetic targeting with ultrasound-induced release of an active agent. The results shown here may be taken as a first step in demonstrating the feasibility of such a concept at least in the case of an orthotopic administration. A biodistribution experiment with iodine-125 labelled plasmid DNA (data not shown) demonstrated that the applied magnetobubble dose remained at the administration site for 24 hrs, no matter whether a magnetic field or ultrasound was applied or not. Therefore, one interpretation of our results is as follows: The magnetobubbles used here are transfection-incompetent upon subcutaneous administration. The use of relatively high power ultrasound for several minutes is sufficient to induce the disassembly of magnetobubbles (as found in *in vitro* experiments with J^{125}-labelled pDNA) and possibly to assist tissue penetration. Anyhow, the disassembled bubble components still require magnetic force to warrant sufficiently tight contact with target cells. The use of a magnetic field alone brings magnetobubbles in tight contact with the target cells but is otherwise not required to hold the injected dose in place. The magnetic field alone is insufficient to mediate transfection because it does not mediate magnetobubble disassembly. Only the combination of magnetic field and ultrasound warrants intimate contact to the target cells, bubble disassembly and possibly tissue penetration. A desired side effect of the magnetic field application is that transfection remains confined to the target tissue and does not afflict the underlying muscle.

In conclusion, this study demonstrates a successful VEGF gene therapy by means of magnetobubble magnetofection in a preclinical setting relevant in reconstructive surgery. The perfusion of the oversized skin flap is increased and the necrosis reduced. An increased flap survival size from 50% to 75% of initial flap size was achieved. In this application, magnetofection of acoustically active magnetic microspheres (magnetobubbles) is equally efficient as adenoviral transduction [1], but due to safety and cost considerations probably more relevant for envisaged clinical use. Magnetobubbles as novel drug carriers and 'magnetosonoporation' as a novel method of physical targeting may have strong potential in multiple therapeutic applications. In addition, being gas-filled microcapsules and comprising magnetic iron oxide nanoparticles, magnetobubbles provide the unique opportunity of combining therapy with modern medical diagnostic techniques like ultrasound (Fig. 11) and magnetic resonance imaging.

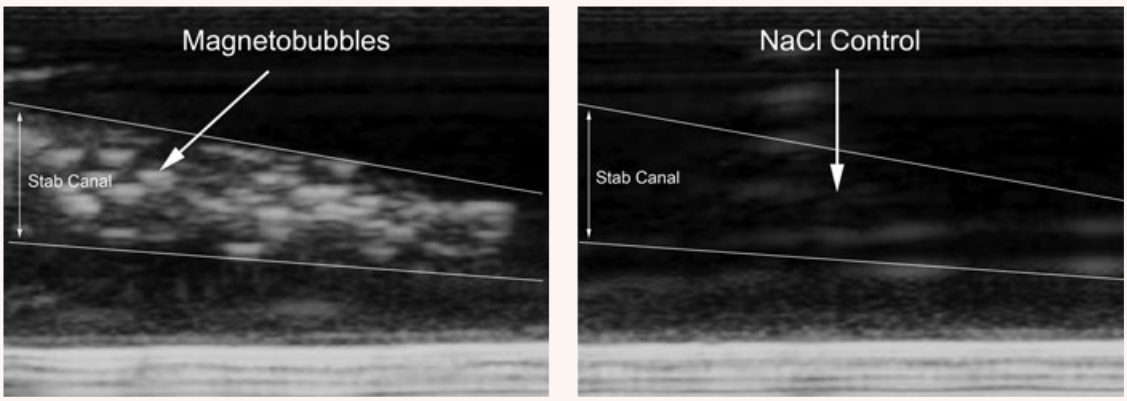

Fig. 11 Ultrasound portrayal. Acoustically active magnetobubbles were pictured in agarose gel *via* ultrasound. No contrast in the stab canal was seen for NaCl, whereas gas-filled magnetobubbles showed the expected contrast. Agarose gel (1%) in TBE (Tris borate)-buffer was prepared with dimensions of 6.5 × 10 cm and 1.3 cm in height. 200–300 μl of magnetic suspension was injected into the agarose gel using a Omnifix®-F single-use syringe and 20G needle (B/Braun AG, Melsungen, Germany). During the lipospheres injection into the gel a video was run showing the lipospheres ultrasound contrast using an ultrasonic device of SIEMENS (VFX 13-5; 10 MHz, 41 dB, Siemens, Germany; depth of penetration: 1 cm). Injection of sodium chloride 0.9% was used as control.

Acknowledgements

The statistical evaluation was performed in cooperation with Dipl. Math. Mrs. Raymonde Busch, Institute of Biomedical Statistics and Epidemiology (Head: Univ.- Prof. Dr. Klaus A. Kuhn), Technische Universität München, Munich. This study was supported by research grants from the 'Deutsche Forschungsgemeinschaft' (DFG), Bonn, Germany (grant #: GI375/3-1) and from the German Federal Ministry of Education and Research (grant #13N8538).

References

1. **Giunta RE, Holzbach T, Taskov C, *et al.*** AdVEGF165 gene transfer increases survival in overdimensioned skin flaps. *J Gene Med*. 2005; 7: 297–306.
2. **Laitinen M, Makinen K, Manninen H, *et al.*** Adenovirus-mediated gene transfer to lower limb artery of patients with chronic critical leg ischemia. *Hum Gene Ther*. 1998; 9: 1481–6.
3. **Laitinen M, Hartikainen J, Hiltunen MO, *et al.*** Catheter-mediated vascular endothelial growth factor gene transfer to human coronary arteries after angioplasty. *Hum Gene Ther*. 2000; 11: 263–70.
4. **Mäkinen K, Manninen H, Hedman M, *et al.*** Increased vascularity detected by digital subtraction angiography after VEGF gene transfer to human lower limb artery: a randomized, placebo-controlled, double-blinded phase II study. *Mol Ther*. 2002; 6: 127–33.
5. **Mann MJ, Whittemore AD, Donaldson MC, *et al.*** Ex-vivo gene therapy of human vascular bypass grafts with E2F decoy: the PREVENT single-centre, randomised, controlled trial. *Lancet*. 1999; 354: 1493–8.
6. **Grines CL, Watkins MW, Helmer G, *et al.*** Angiogenic Gene Therapy (AGENT) trial in patients with stable angina pectoris. *Circulation*. 2002; 105: 1291–7.
7. **Sylvén C, Sarkar N, Ruck A, *et al.*** Myocardial Doppler tissue velocity improves following myocardial gene therapy with VEGF-A165 plasmid in patients with inoperable angina pectoris. *Coron Artery Dis*. 2001; 12: 239–43.
8. **Kutryk MJ, Foley DP, van den Brand M, *et al.*** Local intracoronary administration of antisense oligonucleotide against c-myc for the prevention of in-stent restenosis: results of the randomized investigation by the Thoraxcenter of antisense DNA using local delivery and IVUS after coronary stenting (ITALICS) trial. *J Am Coll Cardiol*. 2002; 39: 281–7.
9. **Rosengart TK, Lee LY, Patel SR, *et al.*** Angiogenesis gene therapy: phase I assessment of direct intramyocardial administration of an adenovirus vector expressing VEGF121 cDNA to individuals with clinically significant severe coronary artery disease. *Circulation*. 1999; 100: 468–74.
10. **Scherer F, Anton M, Schillinger U, *et al.*** Magnetofection: enhancing and targeting gene delivery by magnetic force *in vitro* and *in vivo*. *Gene Ther*. 2002; 9: 102–9.
11. **Luo D, Saltzman WM.** Enhancement of transfection by physical concentration of DNA at the cell surface. *Nat Biotechnol*. 2000; 18: 893–5.
12. **Gersting SW, Schillinger U, Lausier J, *et al.*** Gene delivery to respiratory epithelial cells by magnetofection. *J Gene Med*. 2004; 6: 913–22.
13. **Unger EC, McCreery TP, Sweitzer RH, *et al.*** Acoustically active lipospheres containing paclitaxel: a new therapeutic ultrasound contrast agent. *Invest Radiol*. 1998; 33: 886–92.
14. **Vlaskou D, Mykhaylyk O, Giunta RE, *et al.*** Magnetic microbubbles: new carriers for

localized gene and drug delivery. *Molecular Therapy*. 2006; 13: 290.

15. **Liu Y, Miyoshi H, Nakamura M.** Encapsulated ultrasound microbubbles: therapeutic application in drug/gene delivery. *J Control Release*. 2006; 114: 89–99.
16. **Giunta RE, Holzbach T, Taskov C, *et al.*** Prediction of flap necrosis with laser induced indocyanine green fluorescence in a rat model. *Br J Plast Surg*. 2005; 58: 695–701.
17. **Holzbach T, Taskov C, Henke J, *et al.*** Evaluation der Perfusion von Lappenplastiken mittels Laserfluoreszenz von Indocyaningrün. *Handchir Mikrochir Plast Chir*. 2005; 37: 396–402.
18. **Mykhaylyk O, Antequera YS, Vlaskou D, *et al.*** Generation of magnetic nonviral gene transfer agents and magnetofection *in vitro*. *Nature protocols*. 2007; 2: 2391–411.
19. **Milton SH.** Pedicled skin-flaps: the fallacy of the length: width ratio. *Br J Surg*. 1970; 57: 502–8.
20. **Holzbach T, Neshkova I, Vlaskou D, *et al.*** Searching for the right timing of surgical delay: angiogenesis, vascular endothelial growth factor and perfusion changes in a skin-flap model. *J Plast Reconstr Aesthet Surg*. 2009; 62: 1534–42.
21. **Chalkley HW.** Method for the quantitative morphologic analysis of tissues. *J Natl Cancer Inst*. 1943; 4: 47–53.
22. **Li C, Gardy R, Seon BK, *et al.*** Both high intratumoral microvessel density determined using CD105 antibody and elevated plasma levels of CD105 in colorectal cancer patients correlate with poor prognosis. *Br J Cancer*. 2003; 88: 1424–31.
23. **Konerding MA, Fait E, Gaumann A.** 3D microvascular architecture of pre-cancerous lesions and invasive carcinomas of the colon. *Br J Cancer*. 2001; 84: 1354–62.
24. **Ravnic DJ, Jiang X, Wolloscheck T, *et al.*** Vessel painting of the microcirculation using fluorescent lipophilic tracers. *Microvasc Res*. 2005; 70: 90–6.
25. **Marcus R, Peritz E, Gabriel KR.** On closed testing procedures with special reference to ordered analysis of variance. *Biometrika*. 1976; 63: 655–60.
26. **O'Toole G, MacKenzie D, Lindeman R, *et al.*** Vascular endothelial growth factor gene therapy in ischaemic rat skin flaps. *Br J Plast Surg*. 2002; 55: 55–8.
27. **Huth S, Lausier J, Gersting SW, *et al.*** Insights into the mechanism of magnetofection using PEI-based magnetofectins for gene transfer. *J Gene Med*. 2004; 6: 923–36.
28. **Noble JG, Lee V, Griffith-Noble F.** Therapeutic ultrasound: the effects upon cutaneous blood flow in humans. *Ultrasound Med Biol*. 2007; 33: 279–85.
29. **Newman CM, Bettinger T.** Gene therapy progress and prospects: ultrasound for gene transfer. *Gene Ther*. 2007; 14: 465–75.